

Four terminal quantum dot as an efficient rectifier of heat and charge currents

Karol I. Wysokiński

*Institute of Physics, M. Curie-Skłodowska University,
pl. M. Curie-Skłodowskiej 1, 20-031 Lublin, Poland*

(Dated: January 31, 2023)

We propose an efficient method of heat rectification in a simple system consisting of a quantum dot asymmetrically coupled to four mutually perpendicular electrodes. In such a device the Hall-like charge and heat currents appear in response to the voltage bias or temperature difference between one pair of electrodes. Even though both longitudinal (along the bias) and Hall-like (perpendicular to the bias) currents are rectified under appropriate conditions, the rectification factor is typically much bigger for the latter currents. This is true for heat and charge flow. The Hall-like currents are predicted to exist in linear as well as non-linear transport regimes and require broken mirror symmetry but not time reversal symmetry. The linear effect exists only in geometry which breaks two inversion symmetries along two pairs of electrically coupled terminals. The proposed system is attainable within current technology and provides novel platform of simultaneous heat and charge management at the nanoscale.

I. INTRODUCTION

A rectifier is a device in which the magnitude of the charge or heat current depends on the sign of the electric or thermal bias. Efficient heat current rectifiers are among the most desirable devices at the nanoscale as they allow for heat management in miniaturised electronic devices. Various geometries and devices have been proposed to reach the goal. An early proposal of nanoscale heat rectification has appeared in the context of molecular electronics [1] and is still debated in the literature [2, 3].

In recent years an increased interest is observed in theoretical analysis and experimental studies of thermal diodes [4]. Besides molecules including those with negative U centers [5], many systems with tuned quantum properties have been proposed as possible rectifiers. These include inter alia recently analysed two terminal junctions with bath particles obeying different particle exchange statistics [6] and the use of quantum entanglement as a possible tool to enhance rectification properties [7]. Also various novel solid state systems and materials have been put forward. These include heterostructures, functionally graded or phase changing normal materials, superconductors, etc. as reviewed recently [8, 9].

In the context of this paper, the rectifying devices based on quantum dots are of special interest [10–23]. They consist of a single or more quantum dots coupled to two external reservoirs. Probably the first experimental demonstration of rectifying properties of a two terminal quantum dot is that in Ref. [24] inferred from the asymmetric line shape of the thermopower. Rectification of both charge and heat currents in the Coulomb blockade regime in the system with two quantum dots has been studied in [20]. In [23] the authors concentrate on heat rectification through quantum dots in the Coulomb blockade regime using master equation approach. They considered two-terminal and four-terminal devices. In the latter case, two coupled quantum dots form a main nanoscopic element in which each of the individual dots

is contacted by two separate terminals.

Quantum dots play an important role in novel electronic devices like single electron transistors [25], heat nano-engines [26] and many more, including building blocks of quantum computers [27, 28]. Quantum dots with large charging energy U , coupled to external metallic leads behave like magnetic impurities in noble metals [29, 30] and at low temperature show Kondo effect [31, 32].

The device we are proposing consists of a single quantum dot tunnel coupled to four normal electrodes in a cross geometry as shown in Fig. (1). Application of the voltage or thermal bias along LR electrodes (i.e. x direction) results in a simultaneous flow of (longitudinal) charge and heat currents between L and R electrodes and also between U and D electrodes (Hall-like currents) if the system breaks mirror symmetry(-ies). A device with non-symmetrical couplings works as an efficient rectifier. The rectification is observed for both currents and directions. If the interaction U of electrons is non-negligible, as it is usually the case in small structures, and if working temperature is low enough, the device allows to study the effect of Kondo correlations on longitudinal and Hall-like currents.

Four terminal nano-junctions with similar geometry have been studied previously. General symmetry properties of phase coherent transport in the presence of magnetic flux were derived in [33]. The same geometry was theoretically analysed in the context of Hall-like currents and resistances [34, 35] taking into account polarisation of electrons and strong spin-orbit interaction in the central region. Wei et al. studied planar four terminal system [36] and found non-linear Hall effect induced by the dipole of Berry curvature. The hybrid structure consisting of a quantum dot contacted by tunnel barriers to four electrodes including two superconducting and two normal leads, allows [37] the control of super-current flowing between a pair of superconducting electrodes by the bias voltage applied to normal electrodes. The cross geometry of the four terminal nano-junction containing

an asymmetric prism-like scatterer has been studied experimentally [38]. Even though our system is different from the experimental one it features similar antisymmetric dependence of the four terminal resistance on the current as discussed below.

We shall analyse two possible boundary conditions: open with floating electrodes U and D and open with flow of Hall-like current. There is no Hall voltage [39] under open boundary conditions. However, the Hall-like currents perpendicular to the direction of the bias exist under closed boundary conditions. These conditions are necessary but not sufficient for the observation of Hall-like currents. Breaking of single or two mirror symmetries is needed. The system with broken symmetries shows rectification properties. The rectification efficiency may attain its maximal possible value equal unity. Tuning the system to such hot spots allows perfect rectification of charge or heat. We hope this property can be verified experimentally as the fabrication of the proposed devices is possible by the present-day technology.

The organisation of the paper is as follows. In Section (II) we describe the studied device and its modelling. Two possible boundary conditions are discussed in (II A) and (II B). The results of numerical calculations presented in Section (III) are followed by the concluding Section (IV). Some detailed calculations of currents flowing in the system and the on-dot Green function are relegated to the Appendices (A) and (B).

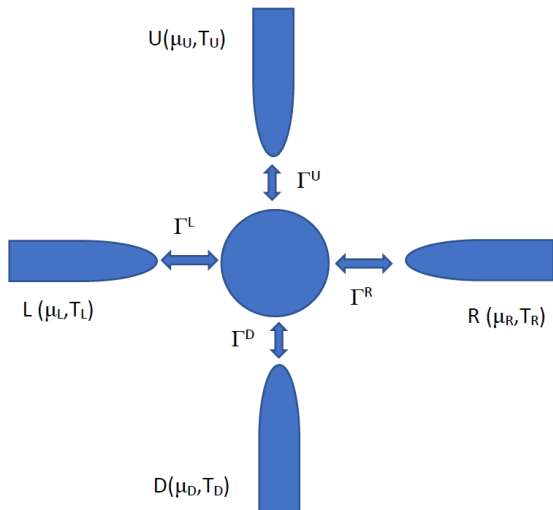


FIG. 1. (color online) The four terminal quantum dot geometry used in this work. The couplings Γ^λ between the central dot and the terminals ($\lambda = L, R, U, D$) take on arbitrary values. The external leads can differ by the chemical potential μ_λ and/or temperature T_λ .

II. THE GEOMETRY, CURRENTS AND BOUNDARY CONDITIONS

The time reversal symmetric nano-structure consisting of a quantum dot tunnel-coupled to four normal leads is illustrated in Fig. (1). The quantum dot is understood here as the small grain with quantized spectrum, which can be modelled by a single level. Electrodes or terminals are macroscopic objects characterised by temperature $T_\lambda = T + \Delta T_\lambda$. They may be electrically biased (eV_λ) with chemical potential $\mu_\lambda = \mu + eV_\lambda$, where μ is an equilibrium value of the chemical potential and T the equilibrium temperature common to all electrodes. We assume $\mu = 0$.

The Hamiltonian describing the system under consideration is a standard single-impurity Anderson model

$$H = \sum_{\lambda k \sigma} \varepsilon_{\lambda k} n_{\lambda k \sigma} + \sum_{\sigma} \varepsilon_{d \sigma} n_{\sigma} + U_d n_{\uparrow} n_{\downarrow} + \sum_{\lambda k \sigma} \left(V_{\lambda k \sigma} c_{\lambda k \sigma}^{\dagger} d_{\sigma} + V_{\lambda k \sigma}^{*} d_{\sigma}^{\dagger} c_{\lambda k \sigma} \right), \quad (1)$$

where $n_{\lambda k \sigma} = c_{\lambda k \sigma}^{\dagger} c_{\lambda k \sigma}$ and $n_{\sigma} = d_{\sigma}^{\dagger} d_{\sigma}$ denote particle number operators for the leads and the dot, respectively. The operators $c_{\lambda k \sigma}^{\dagger}$ (d_{σ}^{\dagger}) create electrons in respective states $\lambda k \sigma$ (σ) in the lead λ (on the dot). The energies of the leads are measured from their chemical potentials μ_λ , $\varepsilon_{\lambda k} = \varepsilon_{0 \lambda k} - \mu_\lambda$, with the dependence of $\varepsilon_{0 \lambda k}$ on λ allowing for a different spectrum in each of the leads. U_d denotes the energy cost of placing two electrons on a quantum dot. In this work we neglect spin dependence of the on dot energy $\varepsilon_{d \sigma} = \varepsilon_d$ and electron hopping amplitudes $V_{\alpha k \sigma} = V_{\alpha k}$. These approximations are relaxed in hybrid system with normal and ferromagnetic electrodes or in the presence of magnetic field. To study the transport properties we employ the non-equilibrium Greens function technique (for details see Appendix (A) and (B)).

A. Absence of Hall voltage in systems with open boundary conditions

We start by assuming the bias B (this denotes either voltage V or temperature ΔT) between L and R electrodes. For open boundary conditions chemical potentials μ_U and μ_D are obtained by requiring that the currents in those electrodes vanish: $I_U = 0$ and $I_D = 0$. Using equations (A2) and (A6) to calculate the currents and neglecting spin dependence it is easy to show that under arbitrary voltage bias V_{LR} the vanishing of charge currents in the U and D electrodes requires

$$F_D - F_U = 0 = \int \frac{dE}{2\pi} (f_D(E) - f_U(E)) N(E). \quad (2)$$

For equal temperatures ($T_D = T_U$) the only solution is $\mu_D = \mu_U$ and no voltage appears along (UD) -direction, regardless the parameters of the model. This is valid for

arbitrary voltages and temperatures, *i.e.* in linear and non-linear regimes. Thus under open boundary conditions there is no 'Hall voltage' in the system and thus no true Hall effect. This, however, does not preclude flow of the Hall currents.

B. The Hall-like current in the four terminal QD with closed boundary conditions

The situation is completely different if one applies closed boundary conditions and allows for a current flow along y-direction. We bias a system along x-direction with $V = V_R - V_L$ or $\Delta T = T_R - T_L$ and calculate the current flow along the UD -direction. It has to be noted that voltage bias induces both, heat J^Q and charge I currents along LR and UD and the same is true for temperature bias. The currents are calculated as $I^{LR} = (I^L - I^R)/2$ and $I^{UD} = (I^U - I^D)/2$ for charge and $J_Q^{LR} = (J_Q^L - J_Q^R)/2$, $J_Q^{UD} = (J_Q^U - J_Q^D)/2$ for a heat flow.

The necessary condition for the existence of currents along unbiased UD direction is broken mirror symmetry between U and D electrodes. This is realised by assuming different couplings to the dot. For symmetric system with $\Gamma^U = \Gamma^D$ the Hall-like currents vanish, $I^{UD} = 0$ ($J_Q^{UD} = 0$). This is easily seen assuming isothermal conditions ($T_\lambda = T$ for all λ) and linear response regime (small voltage $V = V_L - V_R$). For symmetric distribution of voltages $V_{L/R} = \pm V/2$ at the corresponding terminals, one expands the Fermi functions

$$f_\lambda(E) = f_0(E) + f'_0(E)(-eV_\lambda), \quad (3)$$

and using Eq. (A2) gets the Hall-like charge current

$$I^{UD} = \frac{4e^2}{h} \frac{(\Gamma^U - \Gamma^D)[\Gamma^L - \Gamma^R]}{\sum_\lambda \Gamma^\lambda} F'_0 V. \quad (4)$$

where $F'_0 = \int \frac{dE}{2\pi} (-\frac{\partial f_0(E)}{\partial E}) N(E)$. Both currents vanish for $\Gamma^L = \Gamma^R$ and/or $\Gamma^U = \Gamma^D$. This condition is relaxed in the non-linear regime and breaking the mirror symmetry along UD is enough to get the Hall-like currents.

III. THE RESULTS

The asymmetry of couplings plays an important role and in most cases we shall characterise it by a single parameter α , which defines anisotropy of our system. It may take arbitrary positive value but we shall study a few representative values only. In most studied cases we assume simple asymmetry with $\Gamma^R = \Gamma^D = \alpha\Gamma_0$ and $\Gamma^L = \Gamma^U = \Gamma_0$, where Γ_0 is our energy unit. We also assume Boltzmann constant, Planck constant and the electron charge as $k_B = \hbar = e = 1$. Thus energy E and other parameters like T , V and ε_d are all measured in units of Γ_0 .

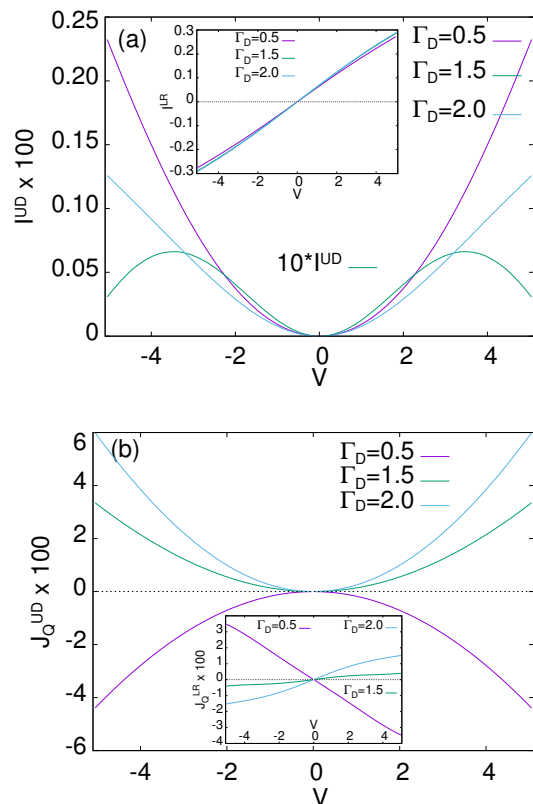


FIG. 2. (color online) Charge current I^{UD} induced by voltage between LR terminals is a symmetric function of V as visible in panel (a). The same is true for heat current which is also symmetric function of voltage (panel b). Insets show the corresponding currents along LR direction. These currents are linear functions at small voltages with non-linear behaviour observed at high bias. Other parameters $T = 1$, $\varepsilon_d = -4$ and $U = 12$.

A. The currents

Contrary to the linear regime in which existence of Hall-like currents require breaking of two mirror symmetries, in the non-linear regime both charge I^{ij} and heat J_Q^{ij} currents flow between $ij = LR$ as well as $ij = UD$ electrodes if only a single mirror symmetry is broken along UD direction. This is illustrated in figure (2) for voltage bias and three values $\Gamma^D = 0.5, 1.5, 2$ with all other couplings equal to $\Gamma_0 = 1$. In accord with Eq. (4) for $\Gamma^L = \Gamma^R$ the linear contributions vanish and the Hall currents are (at least) quadratic functions of voltage for small V . Simultaneously the longitudinal currents (both I^{LR} and J_Q^{LR}) are linear functions of V for $V \rightarrow 0$ with well visible departures from linearity at larger voltages (see insets in Fig. (2) a and b). This agrees with general analytical results of Section (II B). Thermally induced currents (not shown) exhibit the same behaviour, namely the currents perpendicular to the bias are quadratic functions of ΔT for small ΔT . These currents do not appear in the linear order if the system breaks the single mirror

symmetry only. In full analogy to the voltage bias the longitudinal thermally induced currents are linear functions of ΔT for $\Delta T \rightarrow 0$, with departures from linearity at elevated ΔT values.

For the particular set of parameters the UD heat current is positive for $\Gamma^D > 1$ and negative for $\Gamma^D < 1$. This is true independently of the bias as visible from panel (b) in Fig. (2). Similar symmetry is valid for heat currents along LR , which for $\Gamma^D > 1$ are of opposite sign to the currents corresponding to $\Gamma^D < 1$. The flow towards U is either blocked or facilitated.

The response of the system to applied bias quite generally depends on its symmetry and the set of parameters. To illustrate this in Fig. (3) we show thermally induced charge currents in panel (a) and heat currents induced by the voltage in panel (b). Panel (a) shows the currents in system at temperature $T = 2$ with the quantum dot tuned to $\varepsilon_d = -9$, and for two values of anisotropy $\alpha = 0.5, 1.5$ and $U = 12$. The currents flowing along the UD are about an order of magnitude smaller than those along LR direction. However, one notices that the charge Hall - like current for $\alpha = 0.5$ vanishes for $\Delta T/2 \approx 0.4$ but is finite for $\Delta T/2 \approx -0.4$. This is a bias for which the rectification factor is maximal (=1) as we shall see in the following section. In panel (b) we show Hall - like heat currents vs. the voltage. Important fact to note is the non-monotonous dependence of currents on the bias and the points where they vanish. These special points are marked by asterisks.

B. Rectification

If mirror symmetries along LR and UD directions are broken both charge and heat currents in two pairs of electrodes depend on the sign of bias $B = V$ or $B = \Delta T$, i.e. we find $I^{LR}(B) \neq I^{LR}(-B)$ and $I^{UD}(B) \neq I^{UD}(-B)$. The same is true for heat currents $J_Q^{LR}(B)$ and $J_Q^{UD}(B)$. To quantify the rectification efficiency one introduces special parameter called rectification coefficient. One possible definition is

$$R^{ij} = \frac{(|I^{ij}(B)| - |I^{ij}(-B)|)}{(|I^{ij}(B)| + |I^{ij}(-B)|)} \quad (5)$$

With this definition the rectification factor ranges from 0 to 1. The former means no rectification, while the latter perfect rectification. Similar rectification coefficients are defined for heat currents $J^Q(B)$ and we denote them by R_Q^{ij} in the following.

Perfect rectification is expected in cases when the current vanishes for one sign of the bias and attains finite value for the other. The goal is to tune the parameters of the system to such 'hot spots'. In the panel (b) of Fig. (3) such hot spots have been marked by asterisks. The rectification coefficient takes on the maximal possible value at those points. In general it is difficult to tune the system and find vanishing of charge currents.

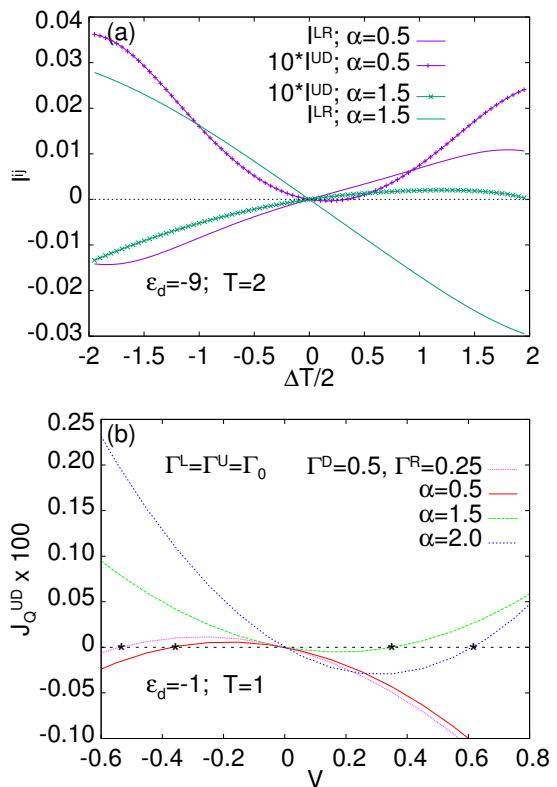


FIG. 3. (color online) In panel (a) we show thermally induced longitudinal charge currents I^{LR} (solid lines) and Hall-like currents I^{UD} (lines with symbols) for two values of asymmetry $\alpha = 0.5$ and $\alpha = 1.5$ as functions of the temperature difference. In the panel (b) the voltage dependent Hall - like heat currents J_Q^{UD} are shown together with points marked with * where the currents vanish for one sign of voltages and take on non-zero values for opposite sign. In both panels $U = 12$.

However, panel (a) of this figure shows points in which Hall-like charge currents vanish for specific values of ΔT . For $\alpha = 0.5$ the I^{UD} current vanishes for $\Delta T/2$ close to 0.4, while for $\alpha = 1.5$ the Hall - like charge current nearly vanishes for $\Delta T/2$ close to 2. In both cases the currents are relatively large for opposite sign of temperature bias.

The rectification coefficients for thermally induced charge and heat currents flowing along LR and UD directions are plotted in Fig. (4). Panel (a) shows R^{ij} for charge currents, while panel (b) R_Q^{ij} for heat currents. The rectification of both currents flowing along the bias direction (I^{LR} and J_Q^{LR}) is relatively small of order of a few percent. For the parameters of the model presented in the figure, the coefficient R^{UD} is of the same order or slightly higher than R^{LR} . Its maximal value is about 10%. However, the heat rectification coefficient $R_Q^{UD} \gg R_Q^{LR}$ and reaches values higher than 50%. It monotonously increases with ΔT .

Temperature plays an important role in our interacting system, as the Kondo effect sets in at low temperature. To see this we show in Fig. (5) results obtained for the

same system as in Fig. (4) for two vastly different temperatures. We plot rectification factors R^{ij} (main panel) and the charge currents I^{ij} (inset) vs. voltage V for two values of temperature. For lower temperature $T = 0.01$ the Kondo resonances are expected to appear in the density of states. The signature of the Kondo effect is visible in the inset as a strongly increased conductance (the curves with symbols correspond to low temperature) at zero voltage. Strong non-linearities at elevated voltages combined with well visible asymmetry of I^{UD} current (at low $T = 0.01$) for voltage around $|V^*| \approx 1.2$ result in $|I^{UD}(V^*)| = |I^{UD}(-V^*)|$ and vanishing of $R^{UD}(V^*)$ as well as its non-monotonous dependence on voltage. At high temperature $T = 1$ there is no Kondo effect and one obtains continuous increase of rectification with V . The rectification of longitudinal current R^{LR} is affected by the Kondo effect only quantitatively. For the particular set of parameters its low temperature value is roughly doubled with respect to higher temperature but remains low, at the level of a few percent.

The general observation is that typically the rectification factors for longitudinal currents are small of the order of a few percent. This agrees with previous systematic calculations of the rectification factor in [23] in a two terminal single level quantum dot. The rectification factors were small of order of a few percent like those for longitudinal currents in the present work. In our four terminal geometry the rectification factor for the Hall-like currents is usually much higher and may be as large 100%.

In view of the observation [23] that the rectification coefficient for a two level quantum dot attains large value in the two terminal system it would be of interest to extend our four terminal model to two level quantum dot and to study how the longitudinal and Hall-like currents and their rectification factors are affected. This will be studied in a future work.

C. Four terminal resistance in the non-linear regime

For many terminal nano-junctions with currents I^{ij} and voltages V^{kl} measured between various pairs of electrodes one defines [33] the four terminal resistances $R_{ij,kl} = \frac{V^{kl}}{I^{ij}}$. The voltages are applied between terminals k and l and currents measured between terminals i and j . Here we shall calculate resistances for a special couplings which break a mirror symmetry along y direction only. If we assume couplings to L, R and U terminals equal to Γ_0 and only the coupling to $\Gamma^D = (0.5, 1.5, 2)\Gamma_0$ different from others, the resulting symmetry of the model resembles that of the nano-junction earlier studied experimentally [38]. These authors considered a four terminal structure with asymmetric triangular prism-like scatterer placed in its centre. The scatterer effectively blocked the flow of charge from/to one of the terminals. In our case it is the coupling Γ^D which effectively blocks (if < 1) the

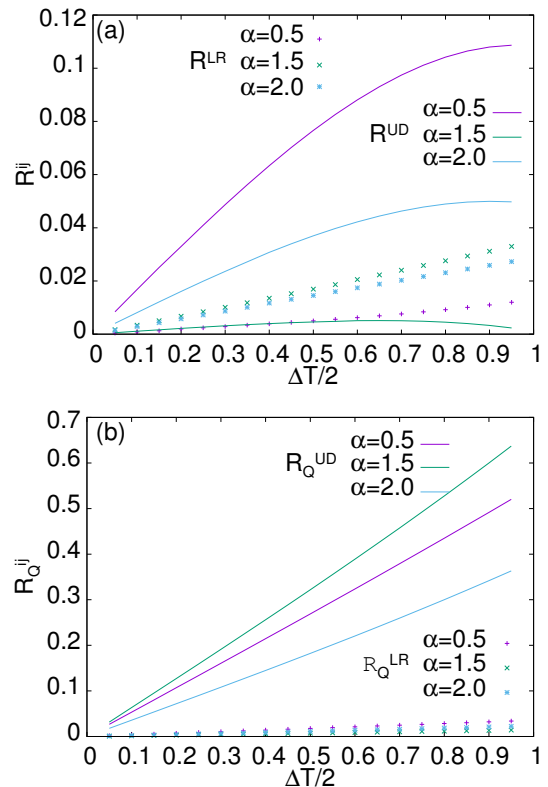


FIG. 4. (color online) Rectification ratios R^{ij} of charge (a) and heat R_Q^{ij} (b) currents as a function of $\Delta T/2$ for a few values of α , voltage $V = 0$, temperature $T = 1$, $\varepsilon_d = -4$ and $U = 12$.

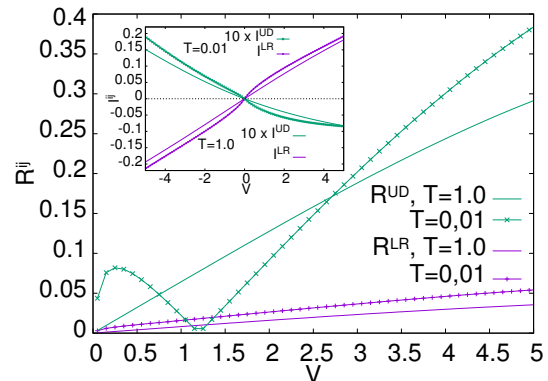


FIG. 5. (color online) Rectification ratios R^{ij} (main panel) and currents I^{ij} (inset) as a function of voltage for two temperatures $T = 1$ (solid lines) and $T = 0.01$ (lines with symbols). Other parameters $\varepsilon_d = -4$ and $U = 12$.

current from/to this terminal.

It should be recalled that in the linear transport regime the resistances $R_{ij,kl}$ do not depend on the current. In the non-linear regime the Hall-like current I^{UD} depends on the longitudinal current I^{LR} and so does the resistance $R_{UD,LR} = \frac{V^{LR}}{I^{UD}} = R_{UD,LR}(I^{LR})$. Due to the van-

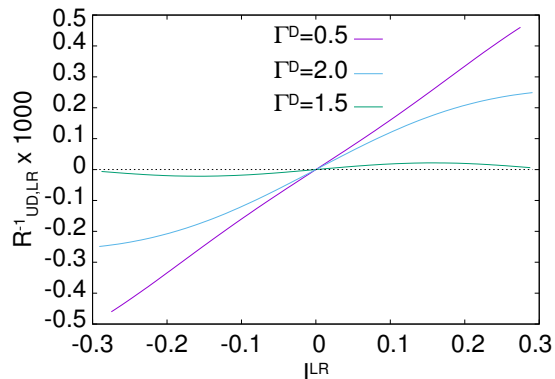


FIG. 6. (color online) Broken mirror symmetry along vertical direction only $\Gamma^R = \Gamma^L = \Gamma^U = 1$ and $\Gamma^D = 0.5, 1.5, 2$ results in the four terminal resistivity antisymmetric with respect to the current flowing along horizontal direction. This resembles experimental result [38] found in the non-linear transport regime of nano-junction with artificial asymmetric scatterer.

ishing of the Hall-like currents at some voltages in our set-up, the four terminal resistance $R_{UD,LR}$ is not well defined at those points. That is why we show in figure (6) the inverse resistance $R_{UD,LR}^{-1} = \frac{I^{UD}}{V^{LR}}$ as a function of the current $I = I^{LR}$. It is seen that the resistance obeys a symmetry $R_{UD,LR}(I) = -R_{UD,LR}(-I)$. Interestingly, similar symmetry of the four terminal resistance has been earlier observed [38] in the non-linear ballistic transport in the (already mentioned) four terminal micro-junction with triangular asymmetric (prism-like) scatterer. The absence of voltage V^{UD} between U and D electrodes in our model and its presence in experimental setup is a main reason of the perfect symmetry $R_{UD,LR}(I) = -R_{UD,LR}(-I)$ in our case and only an approximate one in the nano-junction [38].

Inverse resistances $R_{UD,LR}^{-1}$ calculated in the Kondo regime characterised by the parameters $\varepsilon_d = -4$, $U = 12$ and $T = 0.01$ display the same perfect antisymmetric dependence (not shown) on the longitudinal current I^{LR} . Needless to say that this is true for the mirror symmetry broken along UD direction in a similar way as in experiment [38].

D. Gate voltage dependence and the effect of interactions

In the non-linear regime the density of states (DOS) defined in (A6) and entering formula (A4) is known to depend crucially on the interactions U between carriers, voltages V_λ and temperatures T_λ of the leads. We limit the studies of this section to isothermal condition when all leads have the same temperature $T_\lambda = T$. If temperature is low enough and the on-dot level ε_d is slightly below the chemical potential(s) the Kondo peak(s) appears in the density of states of the interacting quantum

dot. With chemical potentials $\mu = 0$ at electrodes U and D , $\mu_{L/R} = \mu \pm eV/2$ at the left/right electrode one expects three Kondo peaks pinned to the chemical potentials of the electrodes. They are visible in Fig. (9) shown in Appendix (B). Various curves in the figure correspond to different values of $\Gamma^R = \Gamma^D = \alpha\Gamma_0$ couplings with $\Gamma^L = \Gamma^U = \Gamma_0$. For ε_d outside the Kondo regime DOS around $E = 0$ changes smoothly with α and voltage V (not shown).

In figure (7) we show the currents I^{LR} (main panel) and I^{UD} (inset) as function of dot energy ε_d at temperatures below ($T = 0.01$) and above ($T = 0.5$) the Kondo temperature. The dot energy can be easily changed by gate voltage. The system breaks mirror symmetry with respect to both LR and UD directions as we have assumed $\Gamma^L = \Gamma^U = \Gamma_0$ and $\Gamma^R = \Gamma^D = 1.5\Gamma_0$. At lower temperature one observes signatures of the Kondo effect. These are peaks for those gate voltages for which one expects the Kondo resonances in the density of states (c.f. Fig. (9)). The effect is rather small due to the fact that we integrate the density of states over a range $(-V/2, V/2)$ around $E = 0$. In this energy window there are three Kondo peaks including one well pronounced and voltage independent at $E = 0$. It is bounded with the chemical potential $\mu = 0$ of both U and D electrodes. Interestingly, the effect of Kondo correlations is more pronounced in the Hall current I^{UD} as compared to longitudinal one I^{LR} .

In the upper panel of colour coded Fig. (8) we show the dependence of longitudinal I^{LR} charge current on $\delta = \varepsilon_d + U/2$ and voltage V . Lower panel shows similar dependence for the Hall - like charge current I^{UD} . Both currents are calculated for temperature in the Kondo regime ($T = 0.01$) and for $U = 12$. Note, the same scale for both panels, however, with Hall-like current multiplied by the factor of 10.

IV. SUMMARY AND CONCLUSION

We have studied the non-linear transport characteristics of a system consisting of strongly interacting quantum dot coupled to two pairs of normal leads arranged in a cross geometry. The voltage or thermal bias applied to one pair of the leads induces the (heat and charge) current flow between both pairs of terminals, provided the quantum dot is non-symmetrically coupled. Different couplings between the leads and the dot break mirror symmetries of the device. In the linear regime observation of two mutually perpendicular (charge and heat) currents in response to the appropriate bias requires breaking of both symmetries. Beyond linear regime, breaking the mirror symmetry along UD is enough. All currents are rectified in a system breaking both mirror symmetries, with the rectification factors of Hall - like currents typically much bigger than that of longitudinal currents. Interestingly the rectification factor for heat typically exceed that for charge.

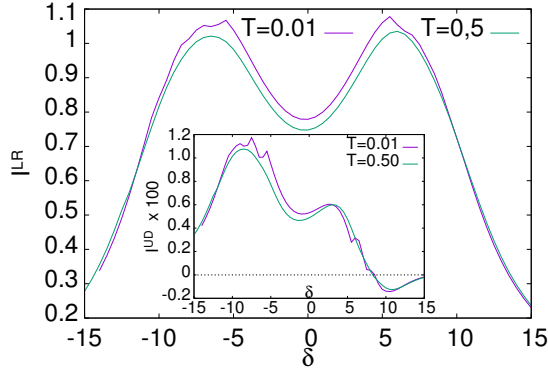


FIG. 7. (color online) The dependence of the longitudinal I^{LR} (main panel) and transverse I^{UD} (inset) currents on the detuning $\delta = \varepsilon_d + U/2$ (can be changed by the gate voltage) for system with $\Gamma^L = \Gamma^U = \Gamma_0$ and $\Gamma^R = \Gamma^D = 1.5\Gamma_0$ (i.e. $\alpha = 1.5$), $U = 16$, voltage bias $V = 4$ and for two temperatures $T = 0.01, 0.5$. Signatures of the Kondo effect visible as non smooth dependence of the currents on δ are observed for $T = 0.01$.

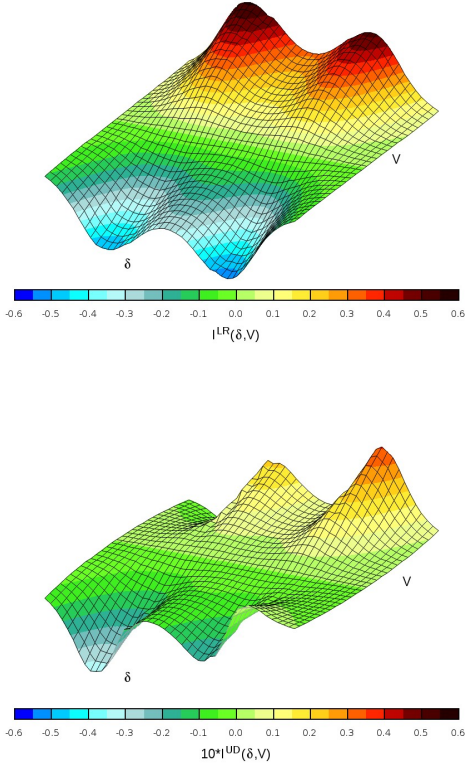


FIG. 8. (color online) The maps show the charge currents on the plane (δ, V) . Upper panel illustrates longitudinal current $I^{LR}(\varepsilon_d, V)$, while lower panel the Hall - like current $I^{UD}(\delta, V)$. We assumed $U = 12$ and temperature $T = 0, 0.01$.

If only the symmetry between Hall leads (perpendicular to those biased) is broken the resulting non-linear four terminal resistance $R_{ij,kl} = \frac{V^{kl}}{I^{ij}}$ is an antisymmetric function of the longitudinal current $I = I^{LR}$, i.e. $R_{UD,LR}(I) = -R_{UD,LR}(-I)$. This is in qualitative agreement with experimental data [38] on non-linear transport in four terminal micro-junction with asymmetric prism - like scatterer. The notable difference is that in our system the anti-symmetry is exact while in experiment it is approximate. It is important to recall that in the linear regime $R_{ij,kl}$ does not depend on the current $I = I^{ij}$.

We want also to underline that the analysed device with a cross geometry enables the study of the Kondo effect on both longitudinal and Hall - like currents. It turns out that the Kondo resonance appearing in the density of states at low temperature affects the longitudinal currents in the four terminal system to lesser extent than in the corresponding two terminal quantum dot geometry. Additionally in our geometry the signatures of the Kondo effect in the Hall - like current are more pronounced than in the longitudinal one.

Our results demonstrate a new route to achieve the efficient rectification of longitudinal and Hall - like (heat and charge) currents. The proposed system is attainable within current technology and provides a novel platform of simultaneous heat and charge management at the nanoscale.

ACKNOWLEDGMENTS

The work reported here has been supported by the M. Curie-Skłodowska University and the National Science Center, Poland (“Weave” programme) through grant no. 2022/04/Y/ST3/00061.

Appendix A: The current in the system

Calculating the currents we follow the general definitions relying on equation of motion of the number and energy operators [40, 41]. The required Green functions are obtained in a standard way [42–44]. Additionally we are assuming the wide band limit when the couplings $\Gamma_\sigma^\lambda(E) = 2\pi \sum_k |V_{\lambda k \sigma}|^2 \delta(E - \varepsilon_{\lambda k}) = \Gamma_\sigma^\lambda$ do not depend on energy. However, we keep here the spin dependence of adequate parameters. In this limit one finds the exact relation (for details see [44, 45])

$$\begin{aligned} \langle d_\sigma^\dagger d_\sigma \rangle &= -i \int \frac{dE}{2\pi} G_\sigma^<(E) \\ &= i \int \frac{dE}{2\pi} \frac{\sum_\lambda \Gamma_\sigma^\lambda f_\lambda(E)}{\sum_\lambda \Gamma_\sigma^\lambda} [G_\sigma^r(E) - G_\sigma^a(E)], \end{aligned} \quad (\text{A1})$$

which allows to write the charge and heat currents flowing out of the λ electrode as

$$I_\lambda = \frac{2e}{\hbar} \int \frac{dE}{2\pi} \sum_\sigma \Gamma_\sigma^\lambda \times \frac{\sum_{\lambda'} \Gamma_{\sigma'}^{\lambda'} (f_{\lambda'}(E) - f_\lambda(E))}{\sum_{\lambda'} \Gamma_{\sigma'}^{\lambda'}} \text{Im} G_\sigma^r(E), \quad (\text{A2})$$

$$J_\lambda = \frac{2e}{\hbar} \int \frac{dE}{2\pi} \sum_\sigma \Gamma_\sigma^\lambda (E - \mu_\lambda) \times \frac{\sum_{\lambda'} \Gamma_{\sigma'}^{\lambda'} (f_{\lambda'}(E) - f_\lambda(E))}{\sum_{\lambda'} \Gamma_{\sigma'}^{\lambda'}} \text{Im} G_\sigma^r(E). \quad (\text{A3})$$

These expressions can be used for calculating the currents in an arbitrary system consisting of the central dot and several terminals under appropriate boundary conditions. Note, the Fermi-Dirac distribution function $f_\lambda(E)$ depends on the electrode λ *via* its chemical potential $\mu_\lambda = \mu + eV_\lambda$ or applied voltage V_λ and temperature T_λ . The common value of the chemical potential and temperature of the system in equilibrium is denoted μ, T . It is convenient to express the currents in terms of auxiliary function

$$F_{\lambda\sigma} = \int \frac{dE}{2\pi} f_\lambda(E) N_\sigma(E), \quad (\text{A4})$$

$$F_{\lambda\sigma}^Q = \int \frac{dE}{2\pi} (E - \mu_\lambda) f_\lambda(E) N_\sigma(E), \quad (\text{A5})$$

respectively. The auxiliary function

$$N_\sigma(E) = -\frac{1}{\pi} \text{Im} G_\sigma^r(E, \{V_\lambda\}) \quad (\text{A6})$$

denotes density of states (DOS) on the dot for spin σ electrons. In general this quantity depends on the voltages $\{V_\lambda\}$ and temperatures T_λ of all terminals.

Appendix B: The Green function

For completeness we recall the formulae for the on-dot Green function which qualitatively correctly describe the Kondo effect. One uses standard equation of motion technique[43–45] and finds the Green function

$$\langle\langle d_\sigma | d_\sigma^\dagger \rangle\rangle_E = \frac{1 + I_d(E) [\langle n_{\bar{\sigma}} \rangle + b_{1\bar{\sigma}} - b_{2\bar{\sigma}}]}{E - \varepsilon_\sigma - \Sigma_{0\sigma} + \Sigma_t(E)}, \quad (\text{B1})$$

where

$$\Sigma_t(E) = I_d(E) [\Sigma_1^T + \Sigma_2^T - (b_{1\bar{\sigma}} - b_{2\bar{\sigma}}) \Sigma_{0\sigma}], \quad (\text{B2})$$

$$I_d(E) = \frac{U}{E - \varepsilon_\sigma - U - \Sigma_{0\sigma} - \Sigma_\sigma^{(1)} - \Sigma_\sigma^{(2)}}. \quad (\text{B3})$$

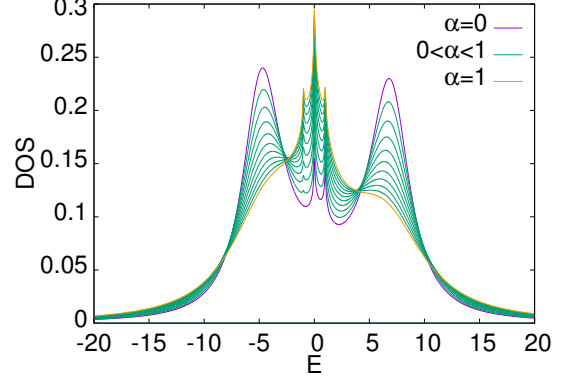


FIG. 9. (color online) The evolution of the on-dot density of states plotted as a function of energy with changing the parameter α describing the couplings between the dot and right (R) and down (D) terminals with $\Gamma^R = \Gamma^D = \alpha\Gamma_0$, $\Gamma^L = \Gamma^U = \Gamma_0$. The parameters take on the following values: the on-dot energy $\varepsilon_d = -5.0$, the source-drain voltage $V = 2$, temperature $T = 0.01$ and the interaction $U = 12$. Note that the region of width V around the chemical potential $\mu = 0$ is important as it contributes to the currents in particular terminals.

The various pieces of the self-energy are supplemented by the inverse life-times $i\gamma_{\bar{\sigma}1/2}$ of the single particle $\bar{\sigma}$, respectively two-particle 2 state and read

$$b_{1\bar{\sigma}}(E) = \int \frac{d\varepsilon}{2\pi} \frac{\sum_\lambda \Gamma_\sigma^\lambda f_\lambda(\varepsilon) \langle\langle d_{\bar{\sigma}} | d_{\bar{\sigma}}^\dagger \rangle\rangle_\varepsilon^a}{E - \varepsilon - \varepsilon_1 + i\tilde{\gamma}_{1\bar{\sigma}}}, \quad (\text{B4})$$

$$b_{2\bar{\sigma}}(E) = \int \frac{d\varepsilon}{2\pi} \frac{\sum_\lambda \Gamma_\sigma^\lambda f_\lambda(\varepsilon) \langle\langle d_{\bar{\sigma}} | d_{\bar{\sigma}}^\dagger \rangle\rangle_\varepsilon^a}{E + \varepsilon - \varepsilon_2 + i\tilde{\gamma}_{2\bar{\sigma}}}, \quad (\text{B5})$$

$$\Sigma_{1\sigma}^T(E) = \int \frac{d\varepsilon}{2\pi} \frac{\sum_\lambda \Gamma_\sigma^\lambda f_\lambda(\varepsilon) [1 + \frac{i}{2} \Gamma_{\bar{\sigma}} \langle\langle d_{\bar{\sigma}} | d_{\bar{\sigma}}^\dagger \rangle\rangle_\varepsilon^a]}{E - \varepsilon - \varepsilon_1 + i\tilde{\gamma}_{1\bar{\sigma}}}, \quad (\text{B6})$$

$$\Sigma_{2\bar{\sigma}}^T(E) = \int \frac{d\varepsilon}{2\pi} \frac{\sum_\lambda \Gamma_\sigma^\lambda f_\lambda(\varepsilon) [1 - \frac{i}{2} \Gamma_{\bar{\sigma}} \langle\langle d_{\bar{\sigma}} | d_{\bar{\sigma}}^\dagger \rangle\rangle_\varepsilon^r]}{E + \varepsilon - \varepsilon_2 + i\tilde{\gamma}_{2\bar{\sigma}}}. \quad (\text{B7})$$

In the above we have introduced $\varepsilon_1 = \tilde{\varepsilon}_\sigma - \tilde{\varepsilon}_{\bar{\sigma}}$, and $\varepsilon_2 = \tilde{\varepsilon}_\sigma + \tilde{\varepsilon}_{\bar{\sigma}} + U$. The subscripts 1 and 2 refer to the excited 1- and 2-electron states of the dot, respectively. The symbols a/r denote advanced/retarded Green function. The self-consistency requires that input dot occupation $\langle n_{\bar{\sigma}} \rangle$ equals that obtained from $G_\sigma^r(E)$ in the consecutive iteration step with a given accuracy. As noted earlier, there exists exact relation

$$\langle n_\sigma \rangle = \int dE \frac{\sum_\lambda \Gamma_\sigma^\lambda f_\lambda(E)}{\sum_\lambda \Gamma_\sigma^\lambda} \left(-\frac{1}{\pi}\right) \text{Im} G_\sigma^r(E), \quad (\text{B8})$$

valid for energy independent couplings; $\Gamma_\sigma^\lambda(E) \equiv \Gamma_\sigma^\lambda$. If this condition is violated, as it might be the case in graphene [46–48], hybrid systems with one (or both) of

the electrodes being a superconductor, *e.g.*, d-wave [49] one, other approaches are needed.

The inverse lifetimes $\tilde{\gamma}_\alpha$ of the excited states $\alpha = |\sigma\rangle, |\uparrow, \downarrow\rangle$ stem from higher order processes [41, 45]. They can be calculated up to the desired order *via* the generalized Fermi rule as

$$\tilde{\gamma}_\alpha = 2\pi \sum_{|f\rangle} |\langle T(E_\alpha) \rangle|^2 \delta(E_\alpha - E_f), \quad (\text{B9})$$

with $T(E) = \hat{V} + \hat{V}g(E)\hat{V} + \dots$ the scattering matrix, where \hat{V} denotes the part of the Hamiltonian describing the coupling between quantum dot and reservoirs. In the discussed approach, one also replaces ε_d by $\tilde{\varepsilon}_d$, to be calculated self-consistently from

$$\tilde{\varepsilon}_d = \varepsilon_d + \Sigma_1^T(\tilde{\varepsilon}_d) + \Sigma_2^T(\tilde{\varepsilon}_d). \quad (\text{B10})$$

Finally, the self-energies $\Sigma_\sigma^{(1,2)}$ are equal to $\Sigma_{0\sigma}$ for $i\tilde{\gamma}_{1,2}^\alpha = i0^+$; however, for arbitrary values of $i\tilde{\gamma}_{1,2}^\alpha$ they

have to be calculated directly from

$$\Sigma_\sigma^{(1,2)}(E) = \sum_\lambda \Gamma_\sigma^\lambda \int \frac{d\varepsilon}{2\pi} \frac{1}{E \mp \varepsilon - \varepsilon_{1,2} + i\tilde{\gamma}_{1,2}^\sigma}. \quad (\text{B11})$$

The on-dot density of states is obtained from the retarded Green function. It is defined by Eq. (A6) and shown in figure (9) as a function of energy for a number of values of the asymmetry factor α (c.f its definition in Section (III)) affecting couplings between the dot and leads. One observes three Abrikosov-Suhl resonances pinned to Fermi levels of the left μ_L , right μ_R and up and down $\mu_U = \mu_D = \mu = 0$ electrodes. Terminal R with $\mu_R = -1.0$ is decoupled from the dot for $\alpha = 0$ so the corresponding density of states shows two Kondo resonances: one at $\mu_U = 0$ and other at $\mu_L = +1.0$. With increasing α the third Kondo resonance appears around energy $E = -1 = \mu_R$. It has to be noted that the Kondo peak at zero energy and two such structures at $V_{L/R}$ make the dependence of currents on gate voltage more complicated in comparison to the two terminal case as the central resonance is always present and only its weight changes with parameters.

-
- [1] Arieh Aviram, Mark A. Ratner, *Molecular rectifiers*, Chemical Physics Letters **29**, 277 (1974).
- [2] Kurt Stokbro, Jeremy Taylor, Mads Brandbyge, *Do Aviram-Ratner Diodes Rectify?* J. Am. Chem. Soc. **125**, 3674 (2003).
- [3] Ioan Baldea, *Why Asymmetric Molecular Coupling to Electrodes Cannot Be at Work in Real Molecular Rectifiers*, Phys. Rev. B **103**, 195408 (2021).
- [4] Hexin Liu, Haidong Wang, Xing Zhang, *A Brief Review on the Recent Experimental Advances in Thermal Rectification at the Nanoscale*, Appl. Sci. **9**, 344 (2019).
- [5] Karol Izydor Wysockiński, *Thermal transport of molecular junctions in the pair tunneling regime*, Phys. Rev. B **82**, 115423 (2010).
- [6] Stephania Palafox, Ricardo Román-Ancheyta, Baris Cakmak, Özgür E. Müstecaplioglu, *Heat transport and rectification via quantum statistical and coherence asymmetries*, Phys. Rev. E **106**, 054114 (2022).
- [7] Kasper Poulsen, Alan C. Santos, Lasse B. Kristensen, Nikolaj T. Zinner, *Entanglement-enhanced quantum rectification*, Phys. Rev. A **105**, 052605 (2022).
- [8] M.Y. Wong, C.Y. Tso, T.C. Ho, H.H. Lee, *A review of state of the art thermal diodes and their potential applications*, International Journal of Heat and Mass Transfer **164**, 120607 (2021).
- [9] F K Malik and K Fobelets, *A review of thermal rectification in solid-state devices*, J. Semicond., **43**, 103101 (2022).
- [10] L. DiCarlo, C. M. Marcus, J. S. Harris, Jr., *Photocurrent, Rectification, and Magnetic Field Symmetry of Induced Current through Quantum Dots*, Phys. Rev. Lett. **91**, 246804 (2003).
- [11] Jesús Iñarrea, Gloria Platero, Allan H. MacDonald, *Electronic transport through a double quantum dot in the spin-blockade regime: Theoretical models*, Phys. Rev. B **76**, 085329 (2007).
- [12] C. R. Müller, L. Worschech, S. Lang, M. Stopa, A. Forchel, *Quantized rectification in a quantum dot nanojunction*, Phys. Rev. B **80**, 075317 (2009).
- [13] David M.-T. Kuo, Yia-chung Chang, *Thermoelectric and thermal rectification properties of quantum dot junctions*, Phys. Rev. B **81**, 205321 (2010).
- [14] Tomi Ruokola, Teemu Ojanen, *Single-electron heat diode: Asymmetric heat transport between electronic reservoirs through Coulomb islands*, Phys. Rev. B **83**, 241404 (2011).
- [15] F. Hartmann, P. Pfeffer, S. Höfling, M. Kamp, L. Worschech, *Voltage Fluctuation to Current Converter with Coulomb-Coupled Quantum Dots*, Phys. Rev. Lett. **114**, 146805 (2015).
- [16] Guillem Rosselló, Rosa López, Rafael Sánchez, *Dynamical Coulomb blockade of thermal transport*, Phys. Rev. B **95**, 235404 (2017).
- [17] Gaomin Tang, Lei Zhang, Jian Wang, *Thermal rectification in a double quantum dots system with a polaron effect*, Phys. Rev. B **97**, 224311 (2018).
- [18] Daniel Malz, Andreas Nunnenkamp, *Current rectification in a double quantum dot through fermionic reservoir engineering*, Phys. Rev. B **97**, 165308 (2018).
- [19] Jincheng Lu, Rongqian Wang, Jie Ren, Manas Kulkarri, Jian-Hua Jiang, *Quantum-dot circuit-QED thermoelectric diodes and transistors*, Phys. Rev. B **99**, 035129 (2019).
- [20] Natalya A Zimbovskaya, *Charge and heat current rectification by a double-dot system within the Coulomb blockade regime*, J. Phys.: Condens. Matter **32**, 325302 (2020).
- [21] A. Iorio, E. Strambini, G. Haack, M. Campisi, F. Giazotto, *Photonic Heat Rectification in a System of Coupled*

- Qubits*, Phys. Rev. Applied **15**, 054050 (2021).
- [22] Y. C. Zhang, S. H. Su, *Thermal rectification and negative differential thermal conductance based on a parallel coupled double quantum-dot*, Physica A **584**, 126347 (2021).
- [23] Ludovico Tesser, Bibek Bhandari, Paolo Andrea Erdman, Elisabetta Paladino, Rosario Fazio, Fabio Taddei, *Heat rectification through single and coupled quantum dots*, New J. Phys. **24**, 035001 (2022).
- [24] Scheibner R, König M, Reuter D, A D Wieck, C Gould, H Buhmann, L W Molenkamp, *Quantum dot as thermal rectifier*, New J Phys, **10**, 083016 (2008).
- [25] M. A. Kastner, *The single-electron transistor*, Rev. Mod. Phys. **64**, 849 (1992).
- [26] G. Benenti, G. Casati, K. Saito, and R. S. Whitney, *Fundamental aspects of steady-state conversion of heat to work at the nanoscale*, Phys. Rep. **694**, 1-124 (2017).
- [27] D. Loss and D. P. DiVincenzo, *Quantum computation with quantum dots*, Phys. Rev. A **57**, 120 (1998).
- [28] G. Burkard, H. A. Engel, and D. Loss, *Spintronics and quantum dots for quantum computing and quantum communication*, Fortschr. Phys. **48**, 965 (2000).
- [29] Tai Kai Ng and Patrick A. Lee, *On-Site Coulomb Repulsion and Resonant Tunneling*, Phys. Rev. Lett. **61**, 1768 (1988).
- [30] L. I. Glazman, M.E. Raikh, *Resonant Kondo transparency of a barrier with quasilocal impurity states*, Pisma Zh. Eksp. Teor. Fiz. **47** 378 (1988) [1988 JETP Lett. **47** 452 (Engl. Transl.)]
- [31] D. Goldhaber-Gordon, H. Shtrikman, D. Mahalu, D. Abush-Magder, U. Meirav, M. A. Kastner, Nature **391**, 156 (1998).
- [32] S. M. Cronenwett, T. H. Oosterkamp, L. P. Kouwenhoven, Science **281**, 540 (1998).
- [33] M. Buttiker, *Four-Terminal Phase-Coherent Conductance*, Phys. Rev. Lett. **57**, 1761 (1986).
- [34] E. N. Bulgakov, K. N. Pichugin, A. F. Sadreev, P. Streda, P. Seba, *Hall-Like Effect Induced by Spin-Orbit Interaction*, Phys. Rev. Lett. **83**, 376 (1999).
- [35] K.N. Pichugin, P. Streda, P. Seba, A.F. Sadreev, *Resonance behaviour of the Hall-like effect induced by spin-orbit interaction in a four-terminal junction*, Physica E **6**, 727 (2000).
- [36] Miaomiao Wei, Bin Wang, Yunjin Yu, Fuming Xu, Jian Wang, *Nonlinear Hall effect induced by internal Coulomb interaction and phase relaxation process in a four-terminal system with time-reversal symmetry*, Phys. Rev. B **105**, 115411 (2022).
- [37] Quin-feng Sun, Jian Wang, Tsung-han Lin, *Control of the supercurrent in a mesoscopic four terminal Josephson junction*, Phys. Rev. B **62**, 648 (2000).
- [38] A. M. Song, A. Lorke, A. Kriele, and J. P. Kotthaus, W. Wegscheider, M. Bichler, *Nonlinear Electron Transport in an Asymmetric Microjunction: A Ballistic Rectifier*, Phys. Rev. Lett. **80**, 3831 (1998).
- [39] N. A. Ashcroft, N. D. Mermin, *Solid State Physics*, 1976.
- [40] Y. Meir and N. S. Wingreen, *Landauer Formula for the current through an interacting electron region*, Phys. Rev. Lett. **68**, 2512 (1992).
- [41] N. S. Wingreen and Y. Meir, *Anderson model out of equilibrium: Noncrossing-approximation approach to transport through a quantum dot*, Phys. Rev. B **49**, 11040 (1994).
- [42] H. Haug and A.-P. Jauho, *Quantum Kinetics in Transport and Optics of Semiconductors, Second, Substantially Revised Edition*, Springer, Berlin, 2008.
- [43] U. Eckern and K. I. Wysokiński, *Two- and three-terminal far-from-equilibrium thermoelectric nanodevices in the Kondo regime*, New J. Phys. **22**, 013045 (2020).
- [44] U. Eckern and K. I. Wysokiński, *Charge and heat transport through quantum dots with local and correlated-hopping interactions*, Phys. Rev. Research **3**, 043003 (2021).
- [45] M. Lavagna, *Transport through an interacting quantum dot driven out-of-equilibrium* J. Phys. Conf. Ser. **592**, 012141 (2015).
- [46] M. M. Wysokiński, *Thermoelectric Effect in the Normal Conductor-Superconductor Junction: A BTK Approach*, Acta Phys. Pol. A **122**, 758 (2012).
- [47] M. M. Wysokiński and J. Spalek, *Seebeck effect in the graphene-superconductor junction*, J. Appl. Phys. **113**, 163905 (2013).
- [48] M. M. Wysokiński, *Temperature Dependence of the Zero-Bias Conductance in the Graphene NIS Junction*, Acta Phys. Pol. A **126**, A36 (2014).
- [49] A. Polkovnikov, *Kondo effect in d-wave superconductors*, Phys. Rev. B **65**, 064503 (2002).